

with  $A(E) = 0$  for  $E > E_c$  and  $B(E) = 0$  for  $E < E_c$ . Values of  $m$  for low  $L$  values are 6 to 10. The observed data exhibit a smoothly changing character from  $L = 2$  to  $L = 10$  with the noteworthy exception of  $L = 6$  (Fig. 4). The more isotropic component of the angular distribution is absent at  $L = 6$ . It is tempting to associate this anomaly with the satellite Io (JI). Io can conceivably inhibit the development of whistler waves in a number of different ways.

Among the various satellite effects that can be identified in the Pioneer 10 and Pioneer 11 data, the most clear-cut and dramatic effect is that caused by Io as shown in Fig. 2 and in larger scale in Fig. 5. The intensities of protons  $0.61 \leq E_p \leq 3.41$  Mev are reduced by a factor of about 100 interior to Io's magnetic shell and the intensities of electrons  $E_e > 40$  kev and  $> 560$  kev are reduced by a factor of about 10 (inbound), whereas the intensities of electrons  $E_e > 21$  and  $> 31$  Mev are only slightly affected.

Full analysis of satellite effects is the most promising technique for understanding the physical dynamics of the magnetosphere of Jupiter, a technique that is not available for the magnetosphere of Earth.

J. A. VAN ALLEN  
B. A. RANDALL  
D. N. BAKER  
C. K. GOERTZ  
D. D. SENTMAN  
M. F. THOMSEN  
H. R. FLINDT

Department of Physics and Astronomy,  
University of Iowa, Iowa City 52242

#### References and Notes

1. J. A. Van Allen, D. N. Baker, B. A. Randall, D. D. Sentman, *J. Geophys. Res.* **79**, 3559 (1974).
2. J. H. Trainor, F. B. McDonald, B. J. Teegarden, W. R. Webber, E. C. Roelof, *ibid.*, p. 3600.
3. R. W. Fillius and C. E. McIlwain, *ibid.*, p. 3589.
4. C. F. Kennel and H. E. Petschek, *ibid.* **71**, 1 (1966).
5. E. J. Smith, L. Davis, Jr., D. E. Jones, P. J. Coleman, Jr., D. S. Colburn, P. Dyal, C. P. Sonett, A. M. A. Frandsen, *ibid.* **79**, 3501 (1974).
6. L. A. Frank, K. L. Ackerson, J. H. Wolfe, J. D. Mihalov, *Univ. Iowa Res. Rep.* 75-5 (January 1975).
7. The work has been supported in large part by contracts NAS2-5603 and NAS2-6553 with the Ames Research Center (ARC) of the National Aeronautics and Space Administration and by contract N00014-68-A-0196-0009 with the Office of Naval Research. We thank in particular C. F. Hall and his Pioneer Project staff at the ARC, and R. F. Randall of the University of Iowa, who designed and developed the electronics of the University of Iowa experiment and supervised and conducted all engineering aspects of the construction and preflight testing and integration into the spacecraft.

14 March 1975

## Jovian Protons and Electrons: Pioneer 11

We present here a preliminary account of the Pioneer 11 passage through the Jovian magnetosphere as viewed by the particle detector systems of the Goddard Space Flight Center and the University of New Hampshire. The detector systems and their operation have been described elsewhere (1, 2). In this report we will restrict our comments almost entirely to the region well within the Jovian magnetosphere, using data from the low energy telescope (LET-II). This detector system measures the proton flux from 0.2 to 21.2 Mev in seven energy intervals and the electron flux from 0.1 to 2 Mev in four intervals. It is well shielded, has a small geometric factor ( $0.015 \text{ cm}^2\text{-ster}$ ), and has an extended dynamic range allowing flux measurements to  $\sim 3 \times 10^7 \text{ cm}^{-2} \text{ sec}^{-1}$ . Representative electron and proton rates (up to  $\sim 2$  Mev) are sampled over eight angular sectors to study particle anisotropies.

In an earlier Pioneer 10 paper (2) we described the Jovian magnetosphere in terms of certain characteristic regions: the region outside the magnetosphere where large fluxes of Mev electrons and protons are observed to be coming from the magnetosphere; the outer Jovian magnetosphere extending from bow shock crossings to  $\sim 50$  Jupiter radii ( $R_J$ ), a region of quasi-trapping and diffusion; a transition region between  $\sim 50$  and  $\sim 25 R_J$ , for example, between the outer diffusion zone and the region where the magnetic field rigidly rotates with the planet; and the region inside  $\sim 25 R_J$ , which

is the really stable trapping region. This is a tentative morphology and is similar to that advanced by the other Pioneer 10 particle experimenters (3). The topology of this magnetosphere which emerges from the results of the particle, magnetic field (4), and plasma (5) measurements is very complicated: it consists of a rapidly rotating, giant magnetosphere which is easily deformed, where the physics is often dominated by a hot plasma inferred but not directly measured by Pioneer; the offset and tilted magnetic field results in a complicated, floppy motion of the magnetic field and the particles within it; and Pioneer 10 results showed quite a different character for this magnetosphere inbound on the sun side, as opposed to the outbound trajectory near the dawn meridian where the electrons and protons were much more concentrated near the equator.

On Pioneer 10, increases of low-energy Jovian electrons (0.2 to 8 Mev) were observed more than 1 astronomical unit (A.U.) away from Jupiter (6). On Pioneer 11 these increases were first observed in January 1974, when the spacecraft was  $\sim 2$  A.U. from the planet. These electron increases persisted over  $\approx 5$ -day periods and tended to recur at 27-day intervals. Furthermore, during the first half of 1974, many of these electron increases were readily detected at 1 A.U. by a more sensitive detector on Interplanetary Monitoring Platform 7. Because of space limitations, these observations will be presented elsewhere. They further

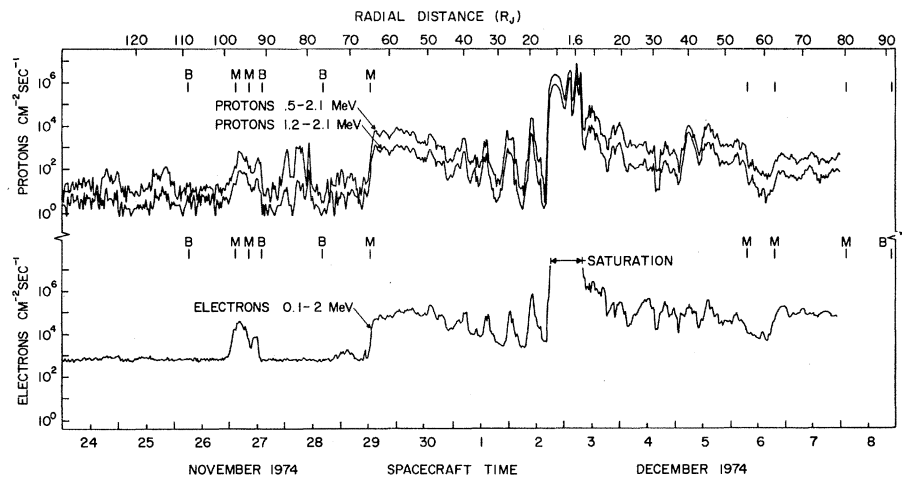


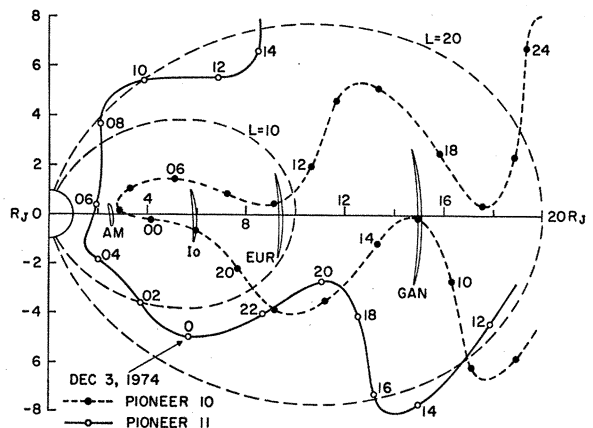
Fig. 1. Fluxes are shown for protons (0.5 to 2.1 Mev and 1.2 to 2.1 Mev) and electrons (0.1 to 2 Mev) for the period 24 November to 8 December 1974. The locations of crossing of the bow shock (B) and magnetopause (M) are noted (12). The relatively high background in this electron measurement from the LET-II telescope amounts to  $\sim 2 \text{ count sec}^{-1}$  and is due to gamma rays from the radioisotope power supply.

confirm that the quiet-time electron increases observed earlier at 1 A.U. are, indeed, of Jovian origin. They suggest that a rather stable interplanetary magnetic field configuration exists over this period, with Jupiter and Earth periodically being close to the same magnetic field lines.

Figure 1 gives an overview of the Pioneer 11 encounter with the Jovian magnetosphere for low-energy protons and electrons. Seen more clearly with our higher-energy detectors, electrons are commonly observed outside the magnetosphere. However, it is evident from Fig. 1 that large fluxes of low-energy protons exist, observed well outside the magnetosphere. On Pioneer 10, low-energy protons were first observed only within a few Jupiter radii of the magnetopause. On Pioneer 11 they are present for days in advance of crossing into the magnetosphere. This is not unexpected, since the outer Jovian magnetosphere is filled with unstably trapped protons and electrons. The continual presence of low-energy solar protons masks the detection of Jovian protons at large distances from the planet.

It is helpful at this point to discuss the relative trajectories of Pioneer 10 and Pioneer 11. Hall (7) describes the Pioneer encounter trajectories as viewed in Jovian local time. Pioneer 10 was on a prograde trajectory, approached Jupiter from a direction approximately  $30^\circ$  west of the Sun, circled the planet in a counterclockwise direction, and exited toward the dawn meridian. Pioneer 11 approached Jupiter from the dawn side, circled the planet clockwise, and exited at high latitudes toward the direction of the Sun. In a simplified view, the inbound trajectory of Pioneer 11 near Jupiter was through the same region of the magnetosphere that Pioneer 10 traversed outbound. Indeed, the clear  $\sim 10$ -hour periodicities and large peak-to-valley ratios seen on Pioneer 11 between  $50 R_J$  and  $20 R_J$  inbound is quite similar to that measured outbound on Pioneer 10. Similarly, the data from Pioneer 10 inbound and Pioneer 11 outbound are qualitatively similar in terms of spectra, angular distributions, and time variations, although the measured fluxes here are consistently much less than those found on Pioneer 10 at lower latitudes. Pioneer 11 measurements in the inner, high-flux region produced verification of the Pioneer 10 results, as well as important new information, and will be discussed in detail later in this report.

Fig. 2. Projection of the trajectories of Pioneer 10 and Pioneer 11 on a magnetic meridian plane of Jupiter based on the  $D_2$  model (4). The region sampled by Pioneer 10 was within  $\sim 20^\circ$  of the magnetic equator, whereas the Pioneer 11 trajectory was at much higher latitudes, usually above  $40^\circ$ . Beyond  $L \sim 10 R_J$  distortions are important, so the  $L = 20$  trace is really an idealization.



It is apparent from Fig. 1 that the low-energy proton spectra changed little between the magnetopause and  $\sim 10 R_J$ . A detailed spectral analysis based on the use of data from the LET-II and LET telescopes (100 keV to 21.2 MeV) shows the same general hardening of the spectrum as seen on Pioneer 10, as one moves from the magnetopause into the central trapping region. However, the spectra measured on Pioneer 11 are always described by a single power law with the index varying slowly from  $\sim 4$  to  $\sim 3$  as we penetrate the magnetosphere. This is in contrast to the inbound Pioneer 10 results closer to the magnetic equator, where the spectra inside  $\sim 40 R_J$  could not be described by a simple power law.

In order to understand the effects measured in the inner core region of the magnetosphere, the "wobble diagrams" shown in Fig. 2 are most useful (8). In this inner region of the magnetosphere, the Pioneer 10 and Pioneer 11 measurements are directly comparable only at two points, both near  $L$  (magnetic shell parameter) = 12. From  $\sim 2000$  on 2 December to  $\sim 0130$  on 3 December, Pioneer 11 was on  $L$  shells  $\sim 12 R_J$  while moving from  $13^\circ$  to  $44^\circ$  south magnetic latitude. Then, while remaining at essentially

constant magnetic latitude, Pioneer 11 traversed  $L$  shells down to  $L = 3.4$  at  $\sim 0445$  when it passed through  $-40^\circ$  magnetic latitude on its way to the equator 1 hour later.

It is of interest to examine in detail the low-energy nucleon component as shown in Fig. 3. On Pioneer 11 the 14.8- to 21.2-MeV protons were found only inside  $15 R_J$  whereas on Pioneer 10 substantial fluxes were first seen at  $\sim 40 R_J$  and a monotonic increase was found inside  $\sim 26 R_J$ . This is quite consistent, however, in view of the point made earlier that Pioneer 11 approached Jupiter from the dawn side, and Pioneer 10 found these higher-energy protons only inside  $\sim 20 R_J$  on the dawn side. The Pioneer 11 outbound fluxes go to zero beyond  $20 R_J$ , but the spacecraft was at very high latitudes. Pioneer 10 and Pioneer 11 data comparisons for both proton energy intervals at  $\sim 1930$  and  $\sim 2200$  (Pioneer 11) show good agreement.

Decreases of a factor of  $\sim 3.6$  in the 14.8- to 21.2-MeV protons were noted both times that Pioneer 11 crossed the orbit of Io, quite similar to the effects noted on Pioneer 10. Much larger Io effects were seen in the 1.2- to 2.1-MeV interval. Small but significant decreases are noted very close to the times of

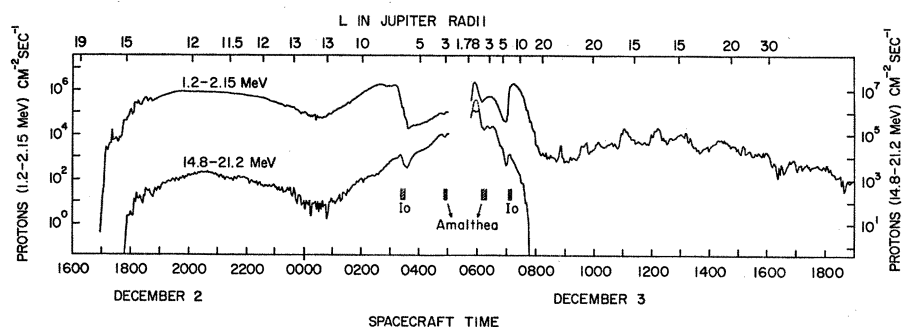


Fig. 3. Flux profiles of 1.2- to 2.15-MeV and 14.8- to 21.2-MeV protons measured in the inner, core region of the Jovian magnetosphere by Pioneer 11. The locations of crossing of Amalthea's orbit from predictions of the  $O_3$  model (9) are shown.

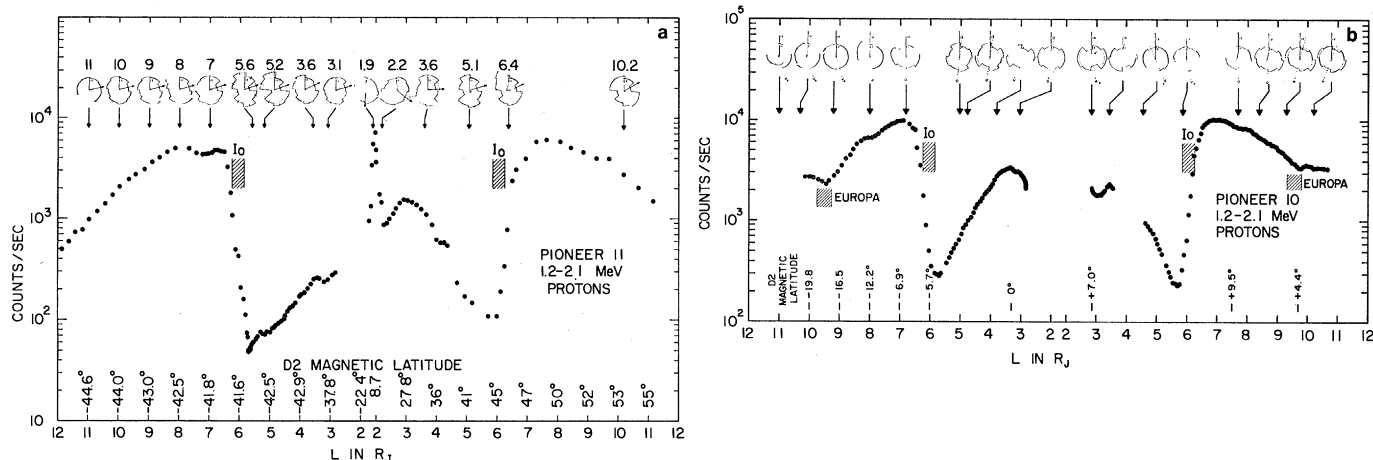


Fig. 4. Count rate data for the 1.2- to 2.1-Mev protons are shown for both Pioneer 10 (b) and Pioneer 11 (a) versus  $L$  calculated from the  $D_2$  model of Jupiter's magnetic field (4). The predicted regions of  $L$  to be swept by Io and Europa are shown. Angular distributions shown are summed in the experiment data system in eight  $45^\circ$  sectors of spin. The detector has a full field view of  $30^\circ$ . The projection of the magnetic field vector on the sector plane is shown.

crossing of Amalthea's orbit, as predicted by the  $O_3$  model of Jupiter's magnetic field (9). In contrast to Pioneer 10, no substantial effects were seen when Pioneer 11 crossed  $L$  shells appropriate to Europa.

A major feature is noted in the Pioneer 11 data at  $L \sim 1.9$ ,  $\lambda_m \sim 6^\circ N$  ( $D_2$  model) where a large, sharp peak in the proton flux occurs. The solid curve shown in Fig. 3 for the 14.8- to 21.2-Mev protons reflects the actual count rates measured, whereas the dashed curve reflects our best estimate of the true fluxes. Saturation of the involved anticoincidence rates were limiting further increase in the 14.8- to 21.2-Mev logical rates. Qualitatively, there are very large fluxes in the nucleonic component at or near the magnetic equator, and the peak fluxes including low-energy alpha particles could be higher by up to a factor of 3 than those estimated ( $\sim 4 \times 10^6$  proton  $\text{cm}^{-2}$   $\text{sec}^{-1}$ ). For similar reasons, the large peak shown in the 1.2- to 2.1-Mev protons is highly suspected of containing many events which should have been logically rejected.

One of the most interesting results from Pioneer 10 was the discovery that Io is able to almost completely remove the lower-energy (1.2 to 2.1 Mev) protons (2). Inbound on Pioneer 11, more than 99 percent of the protons in this energy interval were removed in the  $L$  region which Io occupies. This drop by a factor of  $\sim 100$  compares with a factor of  $\sim 60$  noted with Pioneer 10 data; but Pioneer 11 was at magnetic latitudes above  $40^\circ$ , and the larger effect there is in agreement with predictions (10).

Figure 4 shows the count rate data for 1.2- to 2.1-Mev protons for Pioneer 10 and Pioneer 11 as a function of  $L$  for the  $D_2$  model (4). Angular distributions measured on the spacecraft at the same times are shown at the indicated  $L$  locations. The magnetic latitude ( $D_2$ ) is also indicated periodically, as well as the predicted regions occupied by Europa and Io. The fit of the data for the removal of particles at Io is fair, but the fit lacks to the extent that on both Pioneer 10 and Pioneer 11 the count rates were dropping appreciably at times substantially after the innermost  $L$  shell predicted to be swept by Io. The fit to the  $D_2$  model at Io appears to be better than for the  $O_3$  model (9) inbound at Io; however, no substantial removal of protons while passing through Europa's orbit is apparent from the Pioneer 11 data.

The Pioneer 10 angular distributions have already been discussed, but the Pioneer 11 angular distributions, together with calculations ( $O_3$ ) from Pioneer 11 magnetic field data (11), lead to considerably more insight into these magnetospheric phenomena. Outside  $L \sim 10 R_J$ , the  $O_3$  model calculations (11) show that the loss cone was less than  $5^\circ$  and increased rapidly up to  $\sim 30^\circ$  as Pioneer 11 came across Io's location, decreasing to very small values again as Pioneer 11 moved in and toward the equator. A similar and inverse effect occurred outbound. It seems quite clear that, as the count rate levels off before reaching Io, we are observing the progressive loss of protons into the atmosphere due to the growing loss cone. The effect is even more pronounced at the count rate

minimum inside Io. As Pioneer 11 moved inward further, the loss cone rapidly shrank, the fluxes rapidly increased, and the angular distribution moved toward a more isotropic distribution. An analogous effect was seen as Pioneer 11 moved outbound. The Pioneer 11 data confirm our previous finding that Io permits only  $\sim 1$  percent of the Mev protons to diffuse by its orbit. It also indicates that radical diffusion is the dominant acceleration process in this region for the low-energy nucleons.

In summary, the Pioneer 11 encounter with Jupiter produced most interesting comparisons, contrasts, and new phenomena which will lead to a much better understanding of the Jovian magnetosphere. It is clear that Pioneer 11 was exposed to a much lower total radiation dose than Pioneer 10, largely as a result of the retrograde trajectory which approached and exited the inner region of the magnetosphere at high latitudes. The Pioneer 11 mission has shown that a Jovian-orbiting satellite in a highly inclined orbit could have a reasonable lifetime before radiation damage effects become a problem. This is most important because it could ultimately allow orbits through the magnetotail region where controlling phenomena probably occur.

J. H. TRAINOR, F. B. McDONALD  
D. E. STILWELL, B. J. TEEGARDEN  
*Laboratory for High Energy  
Astrophysics, NASA/Goddard Space  
Flight Center, Greenbelt,  
Maryland 20771*

W. R. WEBBER  
*Space Science Center, University of  
New Hampshire, Durham 03824*

## References and Notes

1. J. H. Trainor, B. J. Teegarden, D. E. Stilwell, F. B. McDonald, E. C. Roelof, W. R. Webber, *Science* **183**, 311 (1974); D. E. Stilwell, R. M. Joyce, J. H. Trainor, H. P. White, Jr., G. Streeter, J. Bernstein, *Inst. Electr. Electron. Eng. Trans. Nucl. Sci.* **22** (No. 1), 1 (1975).
2. J. H. Trainor, F. B. McDonald, B. J. Teegarden, W. R. Webber, E. C. Roelof, *J. Geophys. Res.* **79**, 3600 (1974).
3. J. A. Simpson, D. C. Hamilton, R. B. McKibben, A. Mogro-Campero, K. R. Pyle, A. J. Tuzzolino, *ibid.*, p. 3522; R. B. McKibben and J. A. Simpson, *ibid.*, p. 3545; J. A. Van Allen, D. N. Baker, B. A. Randall, D. D. Sentman, *ibid.*, p. 3559; T. G. Northrop, C. K. Goertz, M. F. Thomsen, *ibid.*, p. 3579; R. W. Fillius and C. E. McIlwain, *ibid.*, p. 3589.
4. E. J. Smith, L. Davis, Jr., D. E. Jones, P. J. Coleman, Jr., D. S. Colburn, P. Dyal, C. P. Sonett, A. M. A. Frandsen, *ibid.*, p. 3501.
5. J. H. Wolfe, J. D. Mihalov, H. R. Collard, D. D. McKibbin, L. A. Frank, D. S. Intriligator, *J. Geophys. Res.* **79**, 3489 (1974).
6. B. J. Teegarden, F. B. McDonald, J. H. Trainor, W. R. Webber, E. C. Roelof, *ibid.*, p. 3615; D. L. Chenette, T. F. Conlon, J. A. Simpson, *ibid.*, p. 3551.
7. C. F. Hall, *Science* **188**, 445 (1975).
8. G. D. Mead, *J. Geophys. Res.* **79**, 3487 (1974); ——— and R. E. Sweeney, *Goddard Space Flight Center Doc. No. X-922-74-339* (November 1974).
9. M. Acuna and N. Ness, personal communication.
10. G. D. Mead and W. N. Hess, *J. Geophys. Res.* **78**, 2793 (1973); W. N. Hess, T. J. Birmingham, G. D. Mead, *ibid.* **79**, 2877 (1974).
11. M. Acuna and N. Ness, personal communication.
12. J. H. Wolfe, personal communication.
13. We thank E. J. Smith and his coinvestigators for supplying the magnetic field data for Pioneer 10 and Pioneer 11 from the helium vector magnetometer and M. Acuna and N. Ness for supplying data from the Pioneer 11 high-field, flux-gate magnetometer.

14 March 1975

already reduced by one or two orders of magnitude only  $10^\circ$  from the equator, we had expected very little radiation at higher latitudes.

It may be that the configuration is altered by a local time difference. If so, however, the change must take place across only  $45^\circ$  in rotation from mid-morning to noon. Alternatively, if the high outbound fluxes are caused by a real time change, it would have to be synchronized coincidentally with closest planetary approach, and no such changes were recorded at other times when the spacecraft was in the magnetosphere. If these possibilities are ruled out, it is still not clear that the magnetodisk model must be abandoned, for this model and the higher latitude phenomena may exist side by side. If this is the case, the Pioneer 11 data imply a latitude profile that initially decreases from a maximum at the equator, goes through a minimum, and then increases to a greater maximum at higher latitudes before dropping off again. The physical processes responsible for this latitude stratification and the interaction between these radiation zones are open questions. However this problem is resolved, it is clear that the new measurements at high latitude provide indispensable information regarding the dynamics and configuration of the vast Jovian magnetosphere.

It is natural to investigate the phase of the modulation for clues regarding the magnetospheric model and internal physical processes. The data in Fig. 1b have been filtered to display frequencies near the planetary rotation cycle, and we have included tic marks synchronized to Jupiter's rotation. The tics on the lower border occur at intervals of one Jovian day (9 hours, 55 minutes, 29.37 seconds); the marks on the bottom line indicate when the spacecraft is aligned and antialigned with

## Radiation Belts of Jupiter: A Second Look

**Abstract.** *The outbound leg of the Pioneer 11 Jupiter flyby explored a region farther from the equator than that traversed by Pioneer 10, and the new data require modification or augmentation of the magnetodisk model based on the Pioneer 10 flyby. The inner moons of Jupiter are sinks of energetic particles and sometimes sources. A large spike of particles was found near Io. Multiple peaks occurred in the particle fluxes near closest approach to the planet; this structure may be accounted for by a complex magnetic field configuration. The decrease in proton flux observed near minimum altitude on the Pioneer 10 flyby appears attributable to particle absorption by Amalthea.*

Pioneer 11 traversed Jupiter's magnetosphere almost exactly 1 year after its predecessor, Pioneer 10 (1). The outbound trajectory was farther from the equator than previous passes, and high particle fluxes encountered here challenge the original magnetodisk model of the outer radiation belts.

Figure 1a illustrates the observations. The large peak spans the closest approach to the planet at 0523 on 3 December with the inbound leg to the left and the outbound leg to the right. The low latitude data inbound exhibit modulation at the Jovian rotation rate with intensity maxima near the expected position of the magnetic equator. Crossings of the current sheet, identified by the magnetometer experiment (2), were found to be in coincidence with some of the maxima. These observations are similar to those from Pioneer 10 and are consistent with the magnetodisk model. The outbound pattern is deceptively similar to that near the equator, with strong modulation at the planetary rotation frequency and comparable intensities. However, there were no current sheet crossings (2), and the maxima were higher even than recorded inbound. Such high intensities were not

visualized in the original magnetodisk model.

According to the original model, the energetic radiation is contained in a disklike volume defined by nearly radial lines of force stretched outward by a current sheet at the equator. The tilt of the internal planetary field imparts an up-and-down motion to the current sheet at the planetary rotation frequency, and the modulation of the trapped radiation is caused by this up-and-down motion in conjunction with a very sharp vertical gradient of the trapped radiation. Because the intensity was

Table 1. Zenocentric and magnetic coordinates for particle features in Fig. 3;  $L$ , magnetic shell parameter.

Feature in Fig. 3	Zenocentric coordinates			Magnetic coordinates		
	$R$ ( $R_J$ )	Latitude (deg)	Longitude III (deg)	Model $D_1^*$		Model $O_3^\dagger$
				$L$	Magnetic latitude	$L$
N1	1.76	-38.6	315	2.79	-36.2	2.48
X1	1.62	-24.3	342	2.15	-27.0	1.72
N2	1.60	-18.0	352	1.99	-22.7	1.61
X2	1.63	1.0	18.0	1.77	-8.3	1.61
N3	1.75	13.2	35.1	1.84	2.0	1.79
X3	1.82	18.5	43.3	1.92	6.8	1.93
N4	2.13	31.8	68.7	2.47	20.5	2.56

\* See (8). † See (7).